Available online at www.sciencedirect.com
ScienceDirect
International Journal of Pharmaceutics 345 (2007) 154–162
INTERNATIONAL JOURNAL OF PHARMACEUTICS
www.elsevier.com/locate/ijpharm

Pharmaceutical Nanotechnology

# Encapsulation of moxifloxacin within poly(butyl cyanoacrylate) nanoparticles enhances efficacy against intracellular *Mycobacterium tuberculosis*

K.O. Kisich [a], S. Gelperina [b,*], M.P. Higgins [a], S. Wilson [a], E. Shipulo [b], E. Oganesyan [b], L. Heifets [a]

[a] *National Jewish Medical and Research Center, Denver, Colorado, USA*
[b] *Russian Research Center for Molecular Diagnostics and Therapy, Moscow, Russia*

Received 25 February 2007; received in revised form 20 May 2007; accepted 23 May 2007
Available online 2 June 2007

**Abstract**

Macrophages in the lungs are the most important cell type supporting replication of *Mycobacterium tuberculosis* in humans. The objective of this study was to investigate whether the effect of moxifloxacin against *M. tuberculosis* residing in macrophages could be improved by encapsulation of the drug in the biodegradable nanoparticles, which are known to accumulate in macrophages upon intravenous administration. To accomplish this, moxifloxacin was encapsulated in poly(butyl cyanoacrylate) (PBCA) nanoparticles. Encapsulated moxifloxacin accumulated in macrophages approximately three-fold times more efficiently than the free drug, and was detected in the cells for at least six times longer than free moxifloxacin at the same extracellular concentration. Inhibition of intracellular *M. tuberculosis* growth with encapsulated moxifloxacin was achieved at the concentration of 0.1 μg/ml, whereas the same effect with free MX required a concentration of 1 μg/ml. Nanoparticles observed within the macrophage cytoplasm were distributed throughout the cytoplasm, sometimes in the vicinity of intracellular bacteria.


*Keywords:* Macrophage; Moxifloxacin; *M. tuberculosis*; Nanoparticles; Poly(butyl cyanoacrylate)

## 1. Introduction

Antimicrobial agents, which are effective against *Mycobacterium tuberculosis*, are widely available and relatively inexpensive; however, little progress has been made during the past 40 years in eradicating this scourge from the developing world, where the majority of infections and deaths from tuberculosis occur. Among the impediments to successful eradication of this infection, there are the problems of complexity of treatment (De Cock and Wilkinson, 1995), duration of treatment (Gelband, 2000), side effects (Myers, 2005), and acquisition of drug resistance (Mitchison, 2005).

In particular, the complexity of treatment could potentially be addressed by development of sustained release formulations, requiring less frequent administration. Sustained release formulations also help guard against the acquisition of drug resistance, as there is less chance for missed doses leading to suboptimal drug concentrations in the blood. One approach to sustained release of anti-tuberculosis drugs has been to encapsulate the drugs in polymeric or lipid carriers, including liposomes (Donald et al., 2001), microparticles (Barrow, 2004), and nanoparticles (Sharma et al., 2004).

Another feature of nanocarriers, which makes them potentially useful for the treatment of intracellular infections, including *M. tuberculosis*, is their ability to accumulate in macrophages. These cells, designed to engulf and destroy pathogens, represent a niche for mycobacteria, which evolved strategies to survive within macrophages thus persisting in the body (Mueller and Pieters, 2006). When nanocarriers are administered intravenously, they are actively cleared from the circulation by the mononuclear phagocytic system (MPS) and typically enhance accumulation of the bound drugs in macrophage-rich organs (Gulyaev et al., 1999; Bakker-Woudenberg et al., 2005). As demonstrated by a number of studies, nanoparticle-

* Corresponding author. Tel.: +7 499 242 9146; fax: +7 499 242 9146.
*E-mail address:* gelperina_svetlana@yahoo.com (S. Gelperina).

0378-5173/$ – see front matter © 2007 Elsevier B.V. All rights reserved.
doi:10.1016/j.ijpharm.2007.05.062

mediated targeting of antibiotics to phagocytic cells of the MPS improves their efficacy in the treatment of intracellular infections (reviewed by Pinto-Alphandary et al., 2000).

A fluoroquinolone antibiotic, moxifloxacin is active against *M. tuberculosis* being as potent as rifampin (Gosling et al., 2003). The present study was performed to determine if encapsulation of moxifloxacin within poly(butyl cyanoacrylate) (PBCA) nanoparticles could further enhance its effect against intracellular *M. tuberculosis* in macrophages.

## 2. Materials and methods

### 2.1. Chemicals

*n*-Butyl-2-cyanoacrylate (Sicomet® 6000) was obtained from Sichel-Werke (Hannover, Germany). Moxifloxacin was obtained from Bayer Pharmaceuticals (West Haven, CT, U.S.A.). Middlebrook 7H9 medium was from Fisher Scientific (Pittsburgh, PA, U.S.A.), fetal bovine serum (FBS)—from Hyclone (Logan, UT, U.S.A.). All other chemicals and solvents were of analytical grade and were purchased from Sigma (St. Louis, MO, U.S.A.).

### 2.2. Preparation and characterization of nanoparticles

#### 2.2.1. Preparation of moxifloxacin-loaded PBCA nanoparticles

Moxifloxacin-loaded PBCA nanoparticles (MX-NP) were obtained by anionic polymerisation of *n*-butyl-2-cyanoacrylate in the presence of a drug. A 1% solution of *n*-butyl-2-cyanoacrylate was added by drops to a 0.1% solution of moxifloxacin (MX) and 1% dextran in 0.01 N HCl with constant stirring at 500 rpm. After 3 h, the reaction was finalized by neutralization with 0.1 N NaOH. Then the nanoparticle suspension was filtered through a G 1 glass filter (Schott, Mainz, Germany) and freeze-dried; 3% (w/v) mannitol was added as a cryoprotector. For the *in vitro* experiments, the freeze-dried preparation was reconstituted in water and used without further purification.

#### 2.2.2. Characterization of moxifloxacin-loaded PBCA nanoparticles

The particle size and polydispersity of the size distribution were measured by photon correlation spectroscopy (PCS) using a Coulter Nanosizer N4MD (Coulter Electronics, U.K.). The samples were diluted with purified water and measured at a temperature of 25 °C and scattering angle of 90°.

For determination of encapsulation efficiency, a 200 μl aliquot of the nanoparticle suspension was centrifuged for 20 min at 10,000 × *g* in centrifugal membrane filter devices (Microcon 30 kDa, Millipore, U.S.A.). The concentration of free MX in filtrate was assessed spectrophotometrically at 292 nm.

#### 2.2.3. Release of moxifloxacin from nanoparticles

*In vitro* release kinetics of MX from the nanoparticles was determined using the centrifugal ultrafiltration technique. The lyophilisate obtained from 1 ml of the nanoparticle suspension was redispersed in 1 ml of phosphate-buffered saline (PBS, pH 7.4). The sample was further diluted (1:25) with PBS or RPMI-1640 basal medium to achieve sink conditions and incubated at 37 °C. At the predetermined time points, 0.25 ml aliquots of the solution were transferred to centrifugal filter units (Microcon YM-30, Millipore, Bedford, MA, U.S.A.), and the amount of MX released was measured in the filtrate, as described above. A solution of free MX was used under the same experimental conditions as a control. The volume of the release medium remained constant since each withdrawn sample was replaced immediately with an equal volume of fresh release medium. The amount of MX in the filtrate was then subtracted from the total drug amount in the sample, as determined by quantitative assay after solubilization of the freeze-dried formulation in DMSO. Each experiment was repeated three times.

#### 2.2.4. Preparation of rhodamine B-loaded PBCA nanoparticles

Rhodamine B-loaded PBCA nanoparticles were prepared and characterized, as described above. The concentration of rhodamine B in the reaction medium was 0.6 mg/ml. Rhodamine B loading measured spectrophotometrically at 490 nm was 78%; mean particle size was 587 ± 130 nm.

### 2.3. Cell culture experiments

#### 2.3.1. Macrophages

THP-1 cells (American Type Culture Collection, Manassas, VA) were maintained at 37 °C in RPMI-1640 containing 10% heat inactivated FBS and were passed once per week. In order to induce differentiation into macrophage-like cells, they were diluted to $1 \times 10^6$/ml; phorbol 12-myristate 13-acetate (Sigma) was added to 50 nM, and the cells were incubated for 3 days. Following differentiation, the cells were rinsed with PBS and placed in fresh medium.

#### 2.3.2. Determination of cytotoxicity of free MX, encapsulated MX, and empty nanoparticles in the macrophages

Free or encapsulated MX was added at desired concentrations to fully differentiated THP-1 monolayers in 24-well tissue culture dishes. Empty nanoparticles (placebo) were added to match the concentration of polymer in the wells treated with MX-loaded nanoparticles. The cells were exposed to the formulations for 4 h; then the medium was removed, and the cells were incubated for another 24 h in the fresh medium. After that 200 μl of a 0.4% Trypan blue solution was added to the THP-1 monolayer for 5 min; then the solution was removed, and the cells were counted under the inverted microscope. A minimum of 500 total cells were counted to determine a percentage of live to dead cells.

#### 2.3.3. Test strain

*M. tuberculosis* H37Rv was used as a target strain. Cultures were grown in Middlebrook 7H9 broth for 7–10 days and then diluted to the optical density of MacFarland Standard No. 1. This density of bacteria equates to approximately $1 \times 10^8$/ml, as

determined by serial dilution and colony counting. The bacterial suspension was then preserved in 1-ml aliquots at −70 °C until needed for infection.

### 2.3.4. Visualization of M. tuberculosis and nanoparticles in THP-1 cells

For visualization of nanoparticle accumulation in the cells, an aliquot of *M. tuberculosis* was thawed and washed with PBS by successive centrifugation and resuspension. The bacteria were labeled by exposure to 10 μg/ml solution of Oregon Green succinimidyl ester (OGSE) for 30 min at 37 °C; the uncoupled dye was removed by further centrifugation and resuspension. The labeled bacteria were then added to 10,000 differentiated THP-1 cells in 8-well chamber slides (Nalge-Nunc, Naperville, II.) at a 10:1 multiplicity of infection for 1 h. The non-adherent bacteria were removed by rinsing cultures three times with fresh medium and incubating the overnight. The chamber slides were then set on the heated humidified stage of a digital microscope system. Nanoparticles containing rhodamine were added to the culture and image stacks acquired to assess the relative location of cells, nanoparticles, and *M. tuberculosis* at increasing intervals of 5, 10, 20, 40, and 60 min. The cultures were then observed microscopically.

### 2.3.5. Measurement of MX accumulation in THP-1 cells

To determine the intracellular drug accumulation, monolayers of THP-1 derived macrophages in 100 mm dishes were exposed to 0.33, 1.0, 3.3, and 10 μg/ml of MX, either free or encapsulated, for 5, 15, 30, 60, and 120 min. The monolayers were rinsed twice with RPMFsaline (1:1) to remove the extracellular drug. One milliliter of sterile distilled water was added to the plates, and they were exposed to three freeze–thaw cycles in order to lyse the cells and release the drug. The lysates were lyophilized and resuspended in 10 μl of PBS for subsequent determination of drug concentration.

### 2.3.6. Bioassay for determination of MX concentration

*Bacillus subtilis* (American type Culture Collection, Manassas, VA) was grown to log phase in LB medium and diluted to $1 \times 10^6$/ml in top agar (0.7% agar, 1% tryptone, 0.5% yeast extract, 0.5% NaCl) held at 37 °C. Five milliliters of the bacteria-top agar suspension was layered over 100 mm LB-agar plates and allowed to cool at room temperature for 1 h. The plates were stored at 4 °C for up to 1 week until needed. To perform an assay of MX, three 6 mm holes were made into the agar using a punch. Known drug concentrations, macrophage lysates, or control solutions were pipetted into the wells in a volume of 50 μl, and the plates were incubated at 37 °C overnight. The diameter of the clear zone was then measured, and a standard curve of MX concentration versus clear zone created. The concentration of MX in macrophage lysates was then interpolated from the diameter of clear zones around wells containing the lysates.

### 2.3.7. Determination of nanoparticle-bound MX activity against intracellular M. tuberculosis

To determine the antimicrobial effect against intracellular bacteria, differentiated THP-1 cell monolayers in 24-well culture plates ($5 \times 10^5$ cells per well) were infected with $2.5 \times 10^6$ CFU/ml of *M. tuberculosis* H37Rv. For traditional time-kill analyses, MX, or MX-NP were added to the cultures and remained there for 4 or 8 days until the cells were lysed; the range of MX concentrations was 0.06–0.5 μg/ml.

Pulsed exposure method. After 1 h of incubation, the extracellular bacteria were removed by three consecutive washes with HBSS. After cultivation for 24 h, the infected monolayers were subjected to 2-h exposure of free or nanoparticle-bound MX in the concentrations of 0.1, 1.0, and 10.0 μg/ml. The unassociated drug was removed by washing three times with HBSS. Cultures were then either lysed immediately for determination of viable bacteria or incubated for additional 4–8 days. The viable bacterial counts (CFU/ml) were performed by plating serial dilutions of the cell lysates on Middlebrook 7H11 plates (Hardy Diagnostics, Santa Maria, CA, U.S.A.) and counting the number of colonies after 21 days of incubation at 37 °C.

### 2.3.8. Data analysis

The numbers of bacterial colonies of either free or encapsulated MX recovered from macrophage cultures at each concentration were plotted against the concentrations being applied. These data were fit to curves in EXCEL, seeking a regression coefficient of 0.9 or greater. The concentration of MX, at which the number of bacteria recovered after 4 days of culture matched the number of bacteria present immediately after infection ($T = 0$), was then interpolated from the line equation. This defines the $IC_{99.9}$ for these experiments. The $IC_{99.9}$ was determined in five replicate experiments, and statistical analysis was performed on the five values for free MX and encapsulated MX to determine the average $IC_{99.9}$ for each formulation. The statistical significance of the differences of the means was then tested via the Mest in EXCEL. A *P*-value of less than 0.05 was set as the significance criterion.

## 3. Results

### 3.1. Encapsulation of moxifloxacin in PBCA nanoparticles

The PBCA nanoparticles were prepared by polymerization of *n*-butyl-2-cyanoacrylate (Couvreur et al., 1979; Kreuter, 1983). This monomer is highly reactive; its polymerization in the aqueous media occurs spontaneously and is initiated by the hydroxyl ions of water, so that the elongation of the polymer chains occurs by anionic polymerization (Behan et al., 2001; Vauthier et al., 2003). The rate of polymerization and the process of particle formation may be controlled by the adjustment of the pH with a strong mineral acid such as hydrochloric acid. At pH 2, formation of the nanoparticles is generally completed after 3 h; after this time, the reaction mixture was neutralized by addition of 0.01 N NaOH to ensure complete conversion of the monomer. The polymerization of *n*-butyl-2-cyanoacrylate in the presence of MX resulted in encapsulation of 44.6 ± 8.3% (41.0–47.6%) of the drug. Average particle size was 418 ± 90.2 nm. The experiment was repeated three times. Overall, the encapsula-

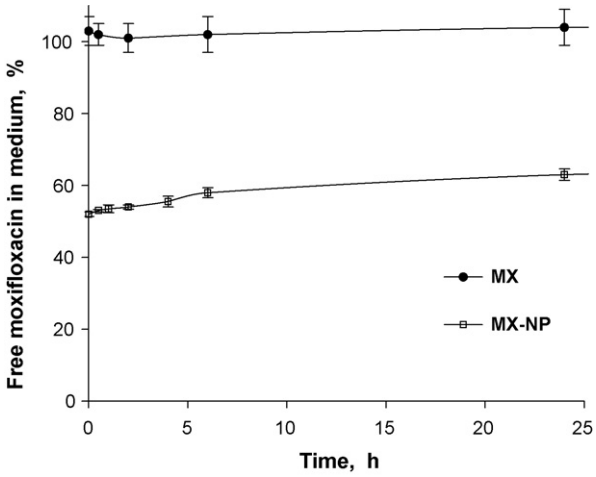


Fig. 1. Efflux kinetics of MX (moxifloxacin) from PBCA nanoparticles. Nanoparticles loaded with MX were resuspended in PBS and rapidly filtered at intervals from 1 min to 24 h (*x*-axis). The concentration of the free drug in the medium is reported on the *y*-axis. The experiment was repeated three times.

tion efficiency varied by 18.6%, while the particle size varied by 21.6%.

In the present study, the attempts to separate a free drug from the nanoparticles by ultrafiltration or ultracentrifugation resulted either in a substantial decrease of loading or in an increase of the particle size and their agglomeration (data not shown). For this reason, the freeze-dried samples of MX-PBCA (as well as the rhodamine-loaded nanoparticles) were used in the cell culture experiments without further purification.

### 3.2. Release of encapsulated moxifloxacin from PBCA nanoparticles

The profile of drug release from PBCA nanoparticles in the PBS medium is shown in Fig. 1. It can be seen that the percentage of the free drug profile immediately reaches 55% (burst release), which is explained by the fact that the formulation initially contained ~55% of the unbound drug. During the steady-state phase the drug concentration was slightly increasing. After 48 h, ~35% of MX was still bound to the nanoparticles. Similar results were obtained when the release was performed in RPMI-1640 medium.

### 3.3. Effect of nanoparticle-encapsulated MX on the viability of cultured macrophages

Exposure of infected macrophages to free MX, encapsulated MX or empty PBCA nanoparticles of comparable size had a dose-dependent effect on the viability of the macrophages (Fig. 3). Free MX caused a slight, non-significant ($P > 0.05$) increase in the number of non-viable (Trypan blue positive) cells at 5 and 10 μg/ml, whereas encapsulated MX was significantly more toxic than a free drug in this concentration range. Empty particles were added into the medium in adequate concentrations and produced a moderate cytotoxic effect at concentrations above 50 μg/ml.

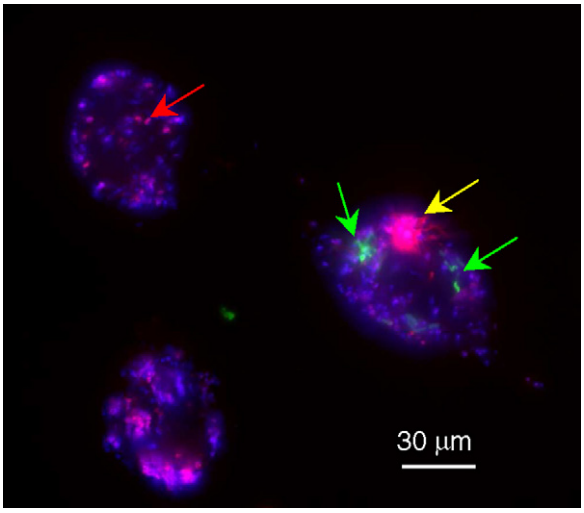


Fig. 2. Distribution of nanoparticles relative to intracellular mycobacteria. Individual macrophages (blue) containing individual rhodamine-loaded nanoparticles (red arrow), and larger aggregates (yellow arrow). Several can be seen in proximity to intracellular *M. tuberculosis* (green arrows). Scale bare equals 30 μm (For interpretation of the references to color in this figure legend, the reader is referred to the web version of the article).

### 3.4. Kinetics and degree of drug accumulation in macrophages

Infected macrophages were exposed to either free or encapsulated MX for increasing time (Fig. 4) or at increasing concentrations (Fig. 5). Macrophages exposed to the MX formulations for increasing time showed a clear and significant difference in accumulation of MX within the cells. This occurred despite only about half of the MX in the formulation was encapsulated in the nanoparticles. While free MX reached a maximum intracellular concentration of 125–175 μg/ml within the first 5 min, encapsulated MX continued to accumulate for the first hour, reaching a maximum intracellular concentration

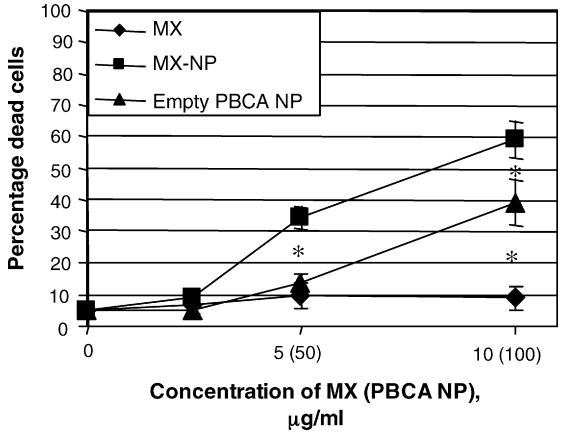


Fig. 3. Toxicity of moxifloxacin, nanoparticle-bound moxifloxacin, and empty PBCA particles for THP-1 macrophages. THP-1 derived macrophages exposed to MX (moxifloxacin) alone (♦), empty PBCA nanoparticles (▲), or MX encapsulated in PBCA nanoparticles (■). The percentage of dead (Trypan blue positive) cells is presented on the *y*-axis, as a function of the amount of MX (or equivalent amount of PBCA alone in parentheses) on the *x*-axis. Error bars represent standard deviation of triplicate wells. $P < 0.05$ by Student's *t*-test (*).

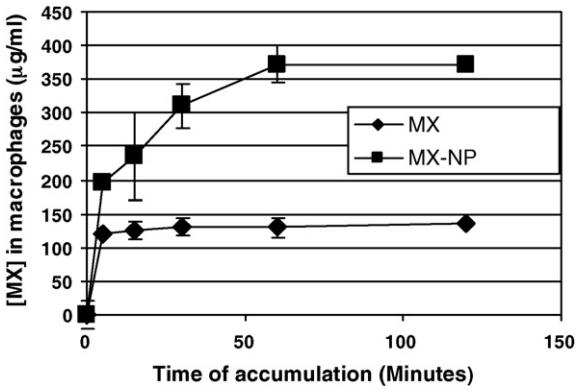


Fig. 4. Kinetics of moxifloxacin accumulation in THP-1 derived macrophages. Macrophages were exposed to 10 μg/ml MX (moxifloxacin) either free in solution (♦), or encapsulated in PBCA nanoparticles (■) for increasing time up to 2 h. The amount of MX within the macrophages was assessed as shown on the *x*-axis.

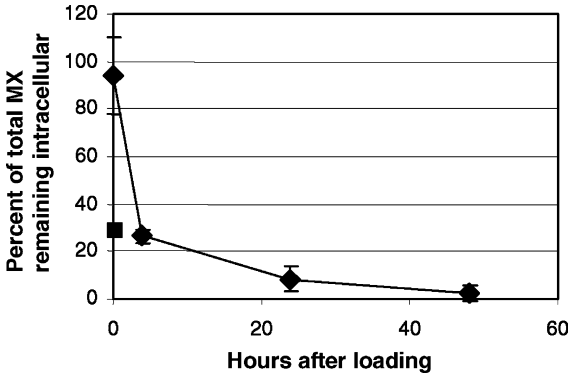


Fig. 6. Efflux of moxifloxacin from macrophages. The fraction of total MX (moxifloxacin) which is intracellular remaining within macrophages is reported after loading with free (■), or nanoparticle-encapsulated MX (♦) (*y*-axis). The values are presented as a function of time after loading (*x*-axis) Error bars represent standard deviation of triplicate samples. The experiment shown is representative of three.

of approximately 375 μg/ml (Fig. 4). The superior accumulation of encapsulated MX in macrophages was highlighted if the experiment was conducted as a function of extracellular concentration, as in Fig. 5. These data show that accumulation of MX in macrophages was much higher at low drug concentration, and the differences become less noticeable when the concentrations were increased. This observation suggests that macrophages are able to accumulate nanoparticulate MX at low concentrations more efficiently than free drug. Possibly, the differences would have been greater if all of the MX in the suspension had been encapsulated; however, as mentioned above, the separation of a free drug from the nanoparticles was not feasible in this study.

Since encapsulated MX could be more efficiently delivered into macrophages, the experiments to determine the kinetic of release of the nanoparticle-bound drug from the cells were also performed. Fig. 6 shows that although the cells lose more than half of the nanoparticle-bound MX within the first 4 h, the drug remains detectable in the cells for at least 24 h. In contrast, free MX was only detectable in the cells immediately after the start of the experiment, falling below the limit of detection within 4 h.

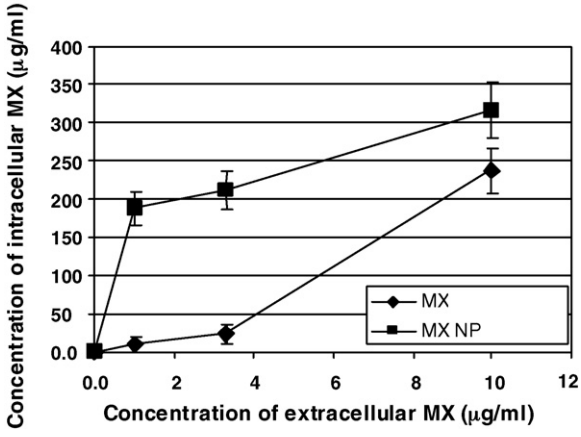


Fig. 5. Concentration dependence of moxifloxacin accumulation within macrophages. Macrophages were exposed to increasing concentrations of free (♦) or encapsulated (■) MX for 1 h as indicated on the *x*-axis. The concentration of MX in the macrophages was then assessed and reported as shown on the *y*-axis.

### 3.5. Accumulation of PBCA nanoparticles within macrophages

The ability of macrophages to accumulate nanoparticles was visualized using fluorescent PBCA nanoparticles labeled with rhodamine B. In order to observe uptake of the particles into macrophages and their distribution in the cells relative to intracellular *M. tuberculosis*, the macrophages were incubated overnight in the presence of *M. tuberculosis* labeled with Oregon Green succinimidyl ester and rhodamine B-loaded nanoparticles. After vigorous washing to remove unassociated mycobacteria and nanoparticles, the cells were examined using a confocal microscope. Fig. 2 illustrates the accumulation of particles within the infected macrophages. Both the particles and the tubercle bacilli were visible within vesicles (most likely phagosomes) in the cytoplasm. The nanoparticles and the mycobacteria appeared to remain in separate compartments, as co-localization between bacteria and particles was not observed. Incubation of the macrophages with the same concentration of unencapsulated rhodamine B did not result in its measurable accumulation within the cells (data not shown).

### 3.6. Effect of MX-loaded nanoparticles on M. tuberculosis within macrophages

The above data suggested that the intracellular concentrations of MX were higher when administered as a nanoparticle formulation relative to free MX, particularly during brief exposures or at low concentration. In order to test the effect of improved accumulation of the encapsulated MX on intracellular *M. tuberculosis*, the effect of encapsulated versus free MX was examined in a traditional assay. Fig. 7 shows that contrary to the hypothesis, encapsulated MX did not perform as well as free MX in this assay. Fig. 8 shows the same data in an effect–concentration–response format, in which the concentra-

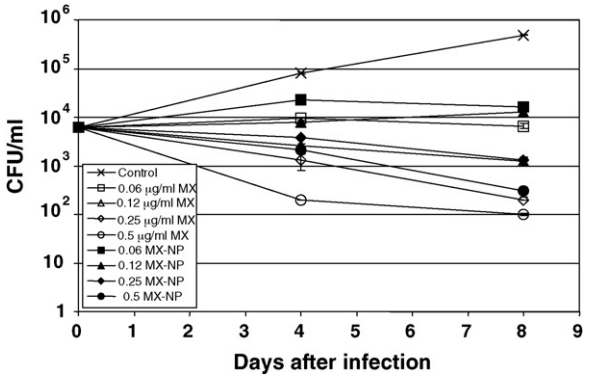


Fig. 7. Time-kill and concentration–response analysis of free vs. encapsulated moxifloxacin. Traditional killing assay for several concentrations of free vs. encapsulated MX (moxifloxacin) at 4 and 8 days after culture setup. Error bars represent standard deviation of triplicate samples. The experiment shown is representative of three.

tion which completely inhibited growth over 8 days ($EC_{99.9}$) was approximately 0.6 μg/ml for free MX and 0.12 μg/ml for encapsulated MX.

For thorough evaluation of the effect of the nanoparticle-bound MX it was tested in a pulsed exposure model. Following establishment of the infection, the cultures were treated for 2 h with free or encapsulated MX at increasing concentrations and then washed to remove unbound drug. The cultures were lysed, and the number of viable bacteria determined by plating on 7H11 agar plates as described. The results are presented in Fig. 9. Relative to controls, cultures treated with 1 μg/ml of either free MX or encapsulated MX had fewer viable *M. tuberculosis* at time 0 (Fig. 9a). The data show significantly greater activity of encapsulated MX relative to free at 0.1, 1.0, and 10 μg/ml (Fig. 9b). Over the course of five concentration–response trials comparing free versus encapsulated MX, the concentration of MX required to inhibit 99.9% of intracellular *M. tuberculosis* growth for 4 days was significantly lower ($P < 0.05$, Student's *t*-test) for encapsulated MX ($3.4 \pm 0.6$ μg/ml), than for free MX ($9.8 \pm 4.6$ μg/ml). Therefore, encapsulation of MX in PBCA nanoparticles enhanced its efficacy against intracellular *M. tuberculosis*; however the advantage is only evident using the pulsed exposure model. The differences between the formulations were more evident at lower concentrations, reflecting the advantage observed in accumulation at lower concentrations for encapsulated MX (Fig. 5).

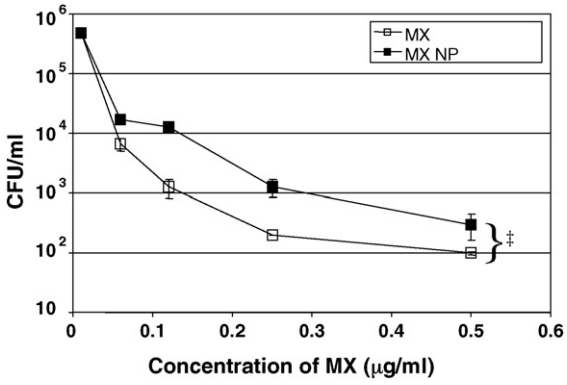


Fig. 8. Concentration–response analysis of free vs. encapsulated moxifloxacin. Day eight data from Fig. 7 were setup in concentration–response format. Multi-regression analysis shows significant difference between the curves ($^{‡}P < 0.001$). Error bars represent standard deviation of triplicate samples. The experiment shown is representative of three.

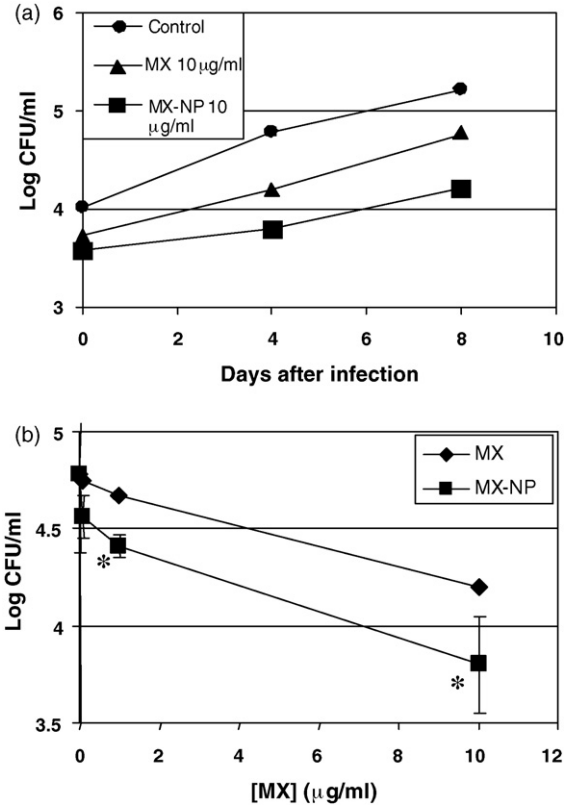


Fig. 9. Effects of nanoparticle-encapsulated MX on intracellular *M. tuberculosis*. Pulse exposure assay: (a) time-kill curve comparing the efficacy of 10 μg/ml free MX (♦) and encapsulated MX (■) against intracellular *M. tuberculosis* vs. untreated cultures (●). (b) Dose–response of free and encapsulated MX for intracellular *M. tuberculosis*. Error bars represent standard deviation of four samples. $P < 0.05$ by Student's *t*-test ($^{*}$).

## 4. Discussion

In the present study, relatively simple and reproducible technology was developed for encapsulation of MX in the nanoparticles made of PBCA, a biocompatible and biodegradable polymer (Vauthier et al., 2003).

The release data suggest that MX is well retained in nanoparticles: >30% of the encapsulated drug was still retained after 48 h incubation at 37 °C. This result correlates with the data obtained by other authors who studied the formulations of fluoroquinolones based on poly(alkyl cyanoacrylate) nanoparticles. Thus, the study of ciprofloxacin release from poly(isobutyl cyanoacrylate) (Fawaz et al., 1997) and poly(ethylbutyl cyanoacrylate) (Page-Clisson et al., 1998) nanoparticles performed under similar experimental conditions demonstrated similar biphasic release profile with 15–40% of the antibiotic still associated with the nanoparticles after 24 h incubation. Poly(ethyl cyanoacrylate) nanoparticles after 24 h release retained ~50–70% of ofloxacin and 15–35% of

pefloxacin (depending on the stabilizer used for nanoparticle preparation) (Fresta et al., 1995).

Whereas release of MX from the nanoparticles in the cell-free media was relatively slow, it could be expected that within the cells the drug release might be facilitated by the enzymatic degradation of the polymeric matrix (Fawaz et al., 1997; Page-Clisson et al., 1998). Indeed, in macrophages MX was released from the particles much more rapidly, as compared to a cell-free medium (Fig. 6). This reflects favorable characteristics of the PBCA particles, which retained the drug-in physiological solutions but released it within the macrophage, which is the target cell for *M. tuberculosis* infection.

The cytotoxicity of the nanoparticles measured in the present study (Fig. 3) correlates with the data of Lherm et al. (1992) who incubated different types of poly(alkyl cyanoacrylate) nanoparticles with L929 fibroblasts and observed a time-dependent increase of the cytotoxicity. This phenomenon was found to be related to the degradation products of polyalkylcyanoacrylates, which are prone to hydrolysis with a formation of water-soluble polycyanoacrylic acid and relative alcohol. Hence, in the present study the cytotoxicity of empty nanoparticles is most probably induced by *n*-butanol released during 24-h period of incubation by the nanoparticles localized intracellularly or adhered to the cell membrane. It has to be mentioned that although the nanoparticles induced certain toxicity *in vitro*, one would expect the much lower toxicity under *in vivo* conditions since the nanoparticles-to-cell ratio used in the *in vitro* experiments presumably is much higher then it would be after *in vivo* administration. In addition, degradation products that are partially or totally responsible for the cytotoxicity of polyalkylcyanoacrylates under *in vivo* conditions are generally eliminated from their site of degradation, thus their contact time with the cells will be considerably lower than *in vitro*. This assumption is supported by the results of toxicological studies performed in rats with a similar nanoparticulate formulation (Gelperina et al., 2002; Pereverzeva et al., 2007). Whereas the cytotoxic effects of the drug and particles were at least additive it was not possible to determine whether these combined effects were greater than additive. Therefore, for evaluation of the effects on survival of intracellular *M. tuberculosis* it may be necessary to take into account the effect of the encapsulated MX on the macrophages themselves.

Loading of MX in the nanoparticles dramatically enhanced the amount of drug associated with the cells (Figs. 4 and 5). While the concentration of free MX within the cells reached its maximum of ~125 μg/ml within 5 min, encapsulated MX continued to accumulate within the cells for the first hour, up to approximately 325 μg/ml. The rapid equilibration of the free drug within the cells suggests that the plasma membrane does not present a significant barrier to drug penetration. These data also suggest that macrophages are able to concentrate free MX approximately 10-fold relative to the extracellular medium, which correlates with the data of Hall et al. (2003).

The enhanced accumulation of encapsulated MX relative to free MX shows that encapsulation allows entry of MX into the cells using an additional cellular internalization process, presumably endocytosis. The nanoparticles are small enough to be taken up via fluid-phase endocytosis, but phagocytosis or macropinocytosis cannot be ruled out.

Initially, the relative efficacy of free versus encapsulated MX was tested by incubation of the formulations with infected cells for the entire 4- or 8-day period. This traditional analysis revealed that encapsulated MX was actually less effective than free MX. Since the same amount of total MX was present in the cultures, it was evident that the intracellular bacteria were exposed to lower concentrations of MX when the drug was encapsulated. Obviously, substantial portion of the drug, which remained associated with the particles during the assay period, was sequestered away from the intracellular bacteria. These results are essentially in agreement with the report of Fawaz et al. (1998) in which ciprofloxacin bound to poly(isobutyl cyanoacrylate) nanoparticles was found to be similar in activity to free ciprofloxacin.

However, the traditional assay does not allow the advantage of detecting the potential depot formulations to become manifest. Indeed, according to the standard procedure the same drug concentration remains in the wells for 8 days unless it is metabolized by the cells. This is not necessarily a good reflection of how macrophages are exposed to drugs *in vivo*, in which the concentration is at its peak for a relatively short time and then declines until the next dose infusion of the drug. Moreover, PBCA nanoparticles are prone to relatively quick degradation and drug release. Therefore, pulsed-exposure format of the assay was designed to achieve more appropriate experimental conditions for the nanoparticle uptake by macrophages. Indeed, under pulsed-exposure format of the assay higher efficacy of encapsulated MX was observed, which is most probably explained by more efficient accumulation of the nanoparticles in the cells (Figs. 4 and 5).

As mentioned above, the difference between the free and encapsulated formulations presumably would have been greater if it had been possible to remove the residual free drug from the nanoparticle formulation. However, this was technically not possible with the type of nanoparticles used in this study. At the same time, similar PBCA-based drug formulations containing both free and bound drug in equilibrium have been studied previously and demonstrated considerably improved pharmacological activity, as compared to free drugs (Kreuter et al., 1995; Steiniger et al., 2004). Accordingly, these formulations are considered to be appropriate for investigation of the mechanism of action and therapeutic potential of the nanoparticles.

The increase in efficacy gained by encapsulation of MX in nanoparticles was a welcome observation. However, based on the increase in accumulation, greater increases in efficacy were expected relative to free drug. There are two possible explanations for this: first, while encapsulated MX may accumulate well in macrophages, a portion of the drug may be sequestered in compartments other than those inhabited by *M. tuberculosis*. This assumption is supported by the data presented in Fig. 2. Indeed, as observed by microscopy, the nanoparticles accumulated well in the macrophages; however, most of the nanoparticles were quite a distance away from *M. tuberculosis* in the macrophage cytoplasm, and only few could be seen in close proximity with intracellular bacteria. Since intracellular

*M. tuberculosis* are reported to reside in vesicles which do not exchange material with the cytoplasm of the cell (Clemens et al., 2002), it is difficult to envision how drug released from particles in distinct phagosomes or lysosomes would gain access to the bacteria.

Another possible explanation for the reduced efficacy relative to the enhanced accumulation is that the additional MX recovered from macrophages may still be associated with nanoparticles. Indeed, the release data obtained in the present study, as well as the data of other authors (Fawaz et al., 1997; Page-Clisson et al., 1998) suggest that fluoroquinolones may interact with alkylcyanoacrylates during the polymerization process, so that a portion of a drug may be covalently bound to the polymeric chain thus becoming inactive. Assuming that MX must be released from the particles in order to affect viability of the bacteria, the effective concentration of active, free drug in the cells would be reduced by the amount still remaining in the particles.

As shown in the present study, free MX was rapidly lost from the macrophages following removal of extracellular MX (Fig. 6). This suggests either diffusion or active transport of MX from the macrophages or degradation/inactivation of the drug by the macrophages. The MX which was lost from the cells was detected in the extracellular medium (data not shown) suggesting that diffusion or efflux was the main route of elimination from the cells. Many human cell types, including leukocytes, are known to have a variety of transporters for the removal of drugs from the cytoplasm (Albermann et al., 2005). It is not known whether any of the drug transporters act to remove MX from cells, but it is an important possibility that would directly impact the effective concentration of MX attainable within macrophages. Therefore, the effective concentration of MX delivered to macrophages in nanoparticles is a function of release rate of the drug from the particles and the rate of drug loss from the cells.

## 5. Conclusions

Encapsulation of moxifloxacin in poly(butyl cyanoacrylate) nanoparticles enhanced its uptake and retention by macrophages, which resulted in increased efficacy of the drug against *M. tuberculosis* residing in macrophages. Further enhancement of efficacy may be realized through targeting of particles to intracellular compartments containing bacteria, and examination of mechanisms by which macrophages remove moxifloxacin from the cytoplasm.

## Acknowledgements

The study was supported by a grant (BII-ISTC #2440) from the BioIndustry Initiative (BII) of the U.S. Department of State and a grant from the U.S. National Institute of Allergy and Infectious Diseases R21 AI 055284-A.

## References

Albermann, N., Schmitz-Winnenthal, F.H., Z'Graggen, K., Volk, C., Hoffmann, M.M., Haefeli, W.E., Weiss, L., 2005. Expression of the drug transporters MDR1/ABCB1, MRP1/ABCC1, MRP2/ABCC2, BCRP/ABCG2, and PXR in peripheral blood mononuclear cells and their relationship with the expression in intestine and liver. Biochem. Pharmacol. 70, 949–958.

Bakker-Woudenberg, L.A., Schiffelers, R.M., Storm, G., Becker, M.J., Guo, L., 2005. Long-circulating sterically stabilized liposomes in the treatment of infections. Methods Enzymol. 391, 228–260.

Barrow, W.W., 2004. Microsphere technology for chemotherapy of mycobacterial infections. Curr. Pharm. Des. 10, 3275–3284.

Behan, N., Birkinshaw, C., Clarke, N., 2001. Poly *n*-butyl cyanoacrylate nanoparticles: a mechanistic study of polymerisation and particle formation. Biomaterials 22, 1335–1344.

Clemens, D.L., Lee, B.Y., Horwitz, M.A., 2002. The *Mycobacterium tuberculosis* phagosome in human macrophages is isolated from the host cell cytoplasm. Infect. Immun. 70, 5800–5807.

Couvreur, P., Kante, B., Roland, M., Guiot, P., Bauduin, P., Speiser, P., 1979. Polycyanoacrylate nanocapsules as potential lysosomotropic carriers: preparation, morphological and sorptive properties. J. Pharm. Pharmacol. 31, 331–332.

De Cock, K.M., Wilkinson, D., 1995. Tuberculosis control in resource-poor countries: alternative approaches in the era of HIV. Lancet 346, 675–677.

Donald, P.R., Sirgel, F.A., Venter, A., Smit, E., Parkin, D.P., Van de Wai, B.W., Mitchison, D.A., 2001. The early bactericidal activity of a low-clearance liposomal amikacin in pulmonary tuberculosis. J. Antimicrob. Chemother. 48, 877–880.

Fawaz, F., Guyot, M., Lagueny, A.M., Devissageut, J.Ph., 1997. Ciprofloxacin-loaded polyisobutylcyanoacrylate nanoparticles: preparation and characterization. Int. J. Pharm. 154, 191–203.

Fawaz, F., Bonini, F., Maugein, J., 1998. Ciprofloxacin-loaded polyisobutylcyanoacrylate nanoparticles: pharmacokinetics and in vitro antimicrobial activity. Int. J. Pharm. 168, 255–259.

Fresta, M., Puglisi, G., Giammona, G., Cavallaro, G., Micali, N., Furneri, P.M., 1995. Pefloxacine mesilate- and ofloxacin-loaded polyethylcyanoacrylate nanoparticles: characterization of the colloidal drug carrier formulation. J. Pharm. Sci. 84, 895–902.

Gelband, H., 2000. Regimens of less than six months for treating tuberculosis. Cochrane Database Syst. Rev. 2, CD001362.

Gelperina, S.E., Khalansky, A.S., Skidan, I.N., Smirnova, Z.S., Bobruskin, A.I., Severin, S.E., Turowski, B., Zanella, F.E., Kreuter, J., 2002. Toxicological studies of doxorubicin bound to polysorbate 80-coated poly(butyl cyanoacrylate) nanoparticles in healthy rats and rats with intracranial glioblastoma. Toxicol. Lett. 126, 131–141.

Gosling, R.D., Uiso, L.O., Sam, N.E., Bongard, E., Kanduma, E.G., Nyindo, M., Morris, R.W., Gillespie, S.H., 2003. The bactericidal activity of moxifloxacin in patients with pulmonary tuberculosis. Am. J. Respir. Crit. Care Med. 168, 1342–1345.

Gulyaev, A.E., Gelperina, S.E., Skidan, I.N., Antropov, A.S., Kivman, G.Y., Kreuter, J., 1999. Significant transport of doxorubicin into the brain with polysorbate 80-coated nanoparticles. Pharm. Res. 16, 1564–1569.

Hall, I.H., Schwab, U.E., Ward, E.S., Ives, T., 2003. Disposition and intracellular levels of moxifloxacin in human THP-1 monocytes in unstimulated and stimulated conditions. Int. J. Antimicrob. Agents 22, 579–587.

Kreuter, J., 1983. Physicochemical characterization of polyacrylic nanoparticles. Int. J. Pharm. 14, 43–58.

Kreuter, L., Alyautdin, R.N., Kharkevich, D.A., Ivanov, A.A., 1995. Passage of peptides through the blood-brain barrier with colloidal polymer particles (nanoparticles). Brain Res. 674, 171–174.

Lherm, C., Mueller, R., Puisieux, F., Couvreur, P., 1992. II. Cytotoxicity of cyanoacrylate nanoparticles with different alkyl chain length. Int. J. Pharm. 84, 13–22.

Mitchison, D.A., 2005. Drug resistance in tuberculosis. Eur. Respir. J. 25, 376–379.

Mueller, P., Pieters, J., 2006. Modulation of macrophage antimicrobial mechanisms by pathogenic mycobacteria. Immunobiology 211, 549–556.

Myers, J.P., 2005. New recommendations for the treatment of tuberculosis. Curr. Opin. Infect. Dis. 18, 133–140.

Page-Clisson, M.E., Pinto-Alphandary, H., Ourevitch, M., Andremont, A., Couvreur, P., 1998. Development of ciprofloxacin-loaded nanoparticles: physicochemical study of the drug carrier. J. Control. Release 56, 23–32.

Pereverzeva, E., Treschalin, I., Bodyagin, D., Maksimenko, O., Langer, K., Dreis, S., Asmussen, B., Kreuter, J., Gelperina, S., 2007. Influence of the formulation on the tolerance profile of nanoparticle-bound doxorubicin in healthy rats: focus on cardio- and testicular toxicity. Int. J. Pharm. 337, 346–356.

Pinto-Alphandary, H., Andremont, A., Couvreur, P., 2000. Targeted delivery of antibiotics using liposomes and nanoparticles: research and applications. Int. J. Antimicrob. Agents 13, 155–168.

Sharma, A., Pandey, R., Sharma, S., Khuller, G.K., 2004. Chemotherapeutic efficacy of poly (DL-lactide-co-glycolide) nanoparticle encapsulated antitubercular drugs at sub-therapeutic dose against experimental tuberculosis. Int. J. Antimicrob. Agents 24, 599–604.

Steiniger, S.C., Kreuter, L., Khalansky, A.S., Skidan, I.N., Bobruskin, A.I., Smirnova, Z.S., Severin, S.E., Uhl, R., Kock, M., Geiger, K.D., Gelperina, S.E., 2004. Chemotherapy of glioblastoma in rats using doxorubicin-loaded nanoparticles. Int. J. Cancer 109, 759–767.

Vauthier, C., Dubernet, C., Fattal, E., Pinto-Alphandary, H., Couvreur, P., 2003. Poly(alkylcyanoacrylates) as biodegradable materials for biomedical applications. Adv. Drug Deliv. Rev. 55, 519–548.